Density of Fe-Ni-C liquids at high pressures and implications for liquid cores of Earth and the Moon

Feng Zhu[1]*, Xiaojing Lai[1,2], Jianwei Wang[3], George Amulele[1,4], Yoshio Kono[5], Guoyin Shen[6], Zhicheng Jing[7], Murli H. Manghnani[1], Quentin Williams[8], Bin Chen[1]*

[1]Hawai'i Institute of Geophysics and Planetology, University of Hawai'i at Mānoa, Honolulu, HI 96822, USA.

[2]Gemmological Institute, China University of Geosciences, Wuhan, Hubei, 430074, China.

[3]Department of Geology and Geophysics, Center for Computation and Technology, Louisiana State University, Baton Rouge, LA 70803, USA.

[4]Department of Earth, Environmental, and Planetary Science, Case Western Reserve University, 10900 Euclid Avenue, Cleveland, OH 44106, USA.

[5]Geodynamics Research Center, Ehime University, Matsuyama, Ehime, 7908577, Japan.

[6]HPCAT, Advanced Photon Source, Argonne National Laboratory, Argonne, IL 60439, USA.

[7]Department of Earth and Space Science, Southern University of Science and Technology, Shenzhen, China.

[8]Department of Earth and Planetary Sciences, University of California, Santa Cruz, Santa Cruz, CA, United States

Corresponding author: Feng Zhu (zhufeng@hawaii.edu), Bin Chen (binchen@hawaii.edu)

Key Points:

- High-pressure density and elasticity of $Fe_{90}Ni_{10}$-3 wt.% C and $Fe_{90}Ni_{10}$-5 wt.% C liquids were determined by experiments and computations
- Compared to liquid Fe, Fe-Ni-C liquids were found to be less compressible and thus possess higher v_p at high pressures
- Carbon can be one of the several major light elements in Earth's outer core, but is unlikely to be the dominant light element in the lunar liquid core

Abstract

The presence of light elements in the metallic cores of the Earth, the Moon, and other rocky planetary bodies has been widely proposed. Carbon is among the top candidates in light of its high cosmic abundance, siderophile nature, and ubiquity in iron meteorites. It is, however, still controversial whether carbon-rich core compositional models can account for the seismic velocity observations within the Earth and lunar cores. Here we report the density and elasticity of $Fe_{90}Ni_{10}$-3 wt.% C and $Fe_{90}Ni_{10}$-5 wt.% C liquid alloys using synchrotron-based X-ray absorption experiments and first-principles molecular dynamics simulations. Our results show that alloying of 3 wt.% and 5 wt.% C lowers the density of $Fe_{90}Ni_{10}$ liquid by ~2.9-3.1% at 2 GPa, and ~3.4-3.6% at 9 GPa. More intriguingly, our experiments and simulations both demonstrate that the bulk moduli of the Fe-Ni-C liquids are similar to or slightly higher than those of Fe-Ni liquids. Thus, the calculated compressional velocity (v_p) of Fe-Ni-C liquids is higher than that of pure Fe-Ni alloy, promoting carbon as a possible candidate to explain the elevated v_p in the Earth's outer core. However, the values and slopes of both density and v_p of the Fe-Ni-C liquids do not match the outer core seismic models, and thus carbon may not be the sole principal element in the outer core. The high v_p of Fe-Ni-C liquids does not match the presumptive v_p of the lunar outer core, indicating that carbon may not be the dominant light element in the lunar outer core.

Plain Language Summary

Light elements such as H, C, O, Si, P and S are considered to be present in the predominantly Fe-Ni liquid cores of the Earth and the Moon. Determining whether a light element is a principal candidate in the core relies chiefly on measuring or calculating the density and sound velocity of the liquid alloys of Fe-Ni and the light element and comparing with results from seismological studies. The controversies in previous studies on the sound velocity of Fe-(Ni)-C liquids have resulted in debates on whether carbon can be the major light element in Earth's or lunar core. In the present study, we combined experiments and theoretical calculations to investigate the density and elasticity of Fe-Ni-C liquids at high pressures. The results show that alloying of carbon lowers the density while increasing the incompressiblity and the sound velocity of Fe-Ni liquids. Compared with the seismological results on the Earth's core, carbon can be a major light element in Earth's liquid core especially if it co-exists with other light elements that lower both the density and sound velocity. Based on current models of the lunar core, our results show that carbon may not be the dominant light element in the moon's liquid core.

1 Introduction

The Earth's core consists predominantly of Fe-Ni alloys [*Birch*, 1952; *Brett*, 1971]. A density deficit of ~10% in the liquid outer core compared with Fe-Ni liquids under similar conditions suggests that there is a considerable amount of light elements, i.e., C, S, P, Si, O, H, alloyed with Fe-Ni [*Li and Fei*, 2014; *Poirier*, 1994]. Light elements are also likely to be present in the cores of other terrestrial bodies such as the Moon, Mercury, Venus, and Mars, given the likely analogous behavior of siderophile elements during planetary accretion and core formation, and particularly iron/silicate partition coefficients of light alloying elements that are likely to be relevant to planetary accretion [*Chen et al.*, 2008; *Fei and Bertka*, 2005; *Jing et al.*, 2014; *Steenstra et al.*, 2017]. The occurrence of Fe-Ni alloys with light elements including C, S, and P in iron meteorites, regarded as fragments of the cores of differentiated planetesimals, also implies the presence of light elements as a general feature within planetary cores. The alloying of light elements may reduce the melting point and electrical and thermal conductivities of Fe-Ni alloys, which are presumably the key to driving the core dynamo and generating an intrinsic magnetic field [*Li and Fei*, 2014]. Therefore, the identity and concentration of light elements in a liquid planetary core is likely pivotal for a terrestrial planet to be protected from the solar wind by a magnetosphere and thus habitable.

Among the top candidate light elements in Earth and planetary cores, carbon has high cosmic abundance, siderophile nature, and ubiquitous occurrence in Fe-Ni meteorites [*Dasgupta and Walker*, 2008; *Wood*, 1993]. Fe-C alloys and Fe carbides, such as Fe_3C and Fe_7C_3, have been widely studied as potential core components in previous studies [*Chen et al.*, 2012; *Chen et al.*, 2018; *Chen et al.*, 2014; *Jiachao Liu et al.*, 2016; *Jin Liu et al.*, 2016; *Lord et al.*, 2009; *Nakajima et al.*, 2011; *Prescher et al.*, 2015]. For Earth's liquid outer core, it remains controversial whether carbon can be a major alloying light element [*Nakajima et al.*, 2015; *Terasaki et al.*, 2010]. Seismic observations of the outer core require light elements to not only reduce the density (ρ), but also elevate the compressional sound velocity v_p ($=\sqrt{K_s/\rho}$, where K_s is the isentropic bulk modulus) of pure Fe [*Poirier*, 1994]. It is well established that the density of Fe-C liquid alloy decreases with increasing carbon concentration at both ambient pressure and high pressures, and the density deficit in Earth's outer core can be accounted for by incorporating certain amount of carbon [*Jimbo and Cramb*, 1993; *Sanloup et al.*, 2011; *Shimoyama et al.*, 2013; *Terasaki et al.*, 2010]. However, *Terasaki et al.* [2010] reported a relatively small isothermal bulk modulus at ambient pressure (K_{T0}) for liquid Fe_3C, arguing that v_p of Fe-C liquid could thus not account for the high v_p of Earth's outer core. Subsequent density measurements on Fe-3.5 wt% C liquid also show a much lower K_{T0} than that of liquid Fe, corroborating this argument [*Shimoyama et al.*, 2013]. Conversely, molecular dynamics simulations reported the bulk moduli of Fe-C liquids with 2.8-5 wt.% C is higher than that of pure liquid Fe [*Belashchenko et al.*, 2011], similar to the relations between solid Fe and Fe-C alloys. Several independent sound velocity measurements also inferred a similar or slightly higher bulk moduli of Fe-C liquids compared to pure Fe [*Kuwabara et al.*, 2016; *Nakajima et al.*, 2015; *Shimoyama et al.*, 2016], contradicting the results from the density measurements [*Shimoyama et al.*, 2013; *Terasaki et al.*, 2010]. Therefore, there is still controversy concerning whether Fe-C liquids can account for both ρ and v_p of the liquid outer core. The disagreement is straightforward, and involves the fundamental question of whether adding carbon to iron-rich liquids results in an elastic stiffening or a softening of liquid iron alloys.

Recently, carbon has also been suggested as the dominant light element in the lunar core, given the metal-silicate partitioning behavior of C and S [*Steenstra et al.*, 2017]. Compared with the Earth, the size and density of the lunar core are still poorly constrained, resulting in difficulties in testing this hypothesis. The Apollo seismic data provides possibly the best anchor point to date, in which the v_p of the lunar liquid core was estimated at ~4.1 km/s [*Weber et al.*, 2011], and its core pressure was calculated at ~5.2 GPa accordingly [*Garcia et al.*, 2012]. This implies that the v_p of the lunar core is lower than that of pure Fe, contrary to the corresponding property in Earth's outer core. Due to the contradictory measurements on K and v_p discussed above, it is difficult to determine whether carbon can be the dominant, or even a plausible, light element in the lunar liquid core.

Here, we combined synchrotron-based X-ray absorption experiments with first-principles molecular dynamics (FPMD) simulations to study the liquid density and elasticity of $Fe_{90}Ni_{10}$ alloyed with 3 wt.% C (hereafter referred to as FeNi-3C) and 5 wt.% C (FeNi-5C) at high pressures and high temperatures. Although the weight percentage of carbon in each composition is not large, the molar percent of carbon (~13 mol% and ~20 mol%, respectively) in each liquid is quite substantial. Combined with previous data, we aim to provide a better assessment of carbon as the major element in the liquid cores of the Earth and the Moon.

2 Materials and Methods

2.1 Synchrotron X-ray absorption experiments

Our starting materials were mixtures of Fe (99.9+%, Sigma-Aldrich), Ni (99.99%, Sigma-Aldrich) and graphite (99.9995%, Alfa Aesar) powders. The mixtures were ground in an agate mortar under acetone for more than 1 h to achieve compositional homogeneity, and then dried in a vacuum oven at high temperature (~383 K) overnight before being sealed in glass vials [*Lai et al.*, 2017].

Experiments were conducted at Beamline 16-BM-B, Advanced Photon Source (APS), Argonne National Laboratory (ANL). A Paris-Edinburgh (P-E) press was employed to achieve high-pressure and high-temperature conditions. For each run, a cold-pressed cylinder-shaped sample (0.8 mm in diameter and 0.4 mm in height) was inserted in a densified Al_2O_3 tube, which was in turn enclosed by a BN (hexagonal boron nitride) sleeve and BN disks. The Pt+MgO (1:10) pressure standard was placed between the BN sleeve and the top BN disk. A densified Al_2O_3 disk with the same diameter as the Al_2O_3 tube was placed above the top BN disk to serve as a reference material in the absorption measurements. Details of the sample assembly are illustrated in Fig. S1.

The sample was first compressed to the target load, and then resistively heated to high temperatures until fully molten. Temperature was determined by the temperature-power curve calibrated in separate experiments using a thermocouple [*Kono et al.*, 2014]. During the first heating cycle of each experiment, the temperature was kept at 1073 K for 90 minutes to sinter the capsule and the sample before attempting higher temperatures. The pressure was determined by energy-dispersive X-ray diffraction (EDXD) measurements on the Pt and MgO pressure markers using a white beam. EDXD data were also collected on the sample every 100 K during continuous heating. The disappearance of all major diffraction peaks of solid phases was used as

the criterion of sample melting (Figure 1). X-ray absorption measurements were then performed on the molten sample as well as the reference Al_2O_3 disk after switching to a monochromatic beam with an energy of 40 keV.

The absorption profiles through the sample and standard were collected by moving the press horizontally and perpendicular to the X-ray beam. The density was determined from X-ray absorption measurements based on the Beer-Lambert law:

$$\frac{I}{I_0} = \exp\left((-\mu\rho t)_{sample} + (-\mu\rho t)_{environment}\right) \quad (1)$$

where I_0 and I are the incident and transmitted X-ray intensities measured by ion chambers placed at the front and rear of the press, respectively, μ – mass attenuation coefficient, ρ – density, and t – thickness, with subscripts indicating sample or environment values. The ion chambers were filled with xenon gas. Given that the measurements on the sample and Al_2O_3 experience the same absorption from surrounding assembly materials (including the Al_2O_3 sample capsule and everything outside it in Fig. S1), we have

$$\frac{I_{sample}}{I_{0sample}} \Big/ \frac{I_{Al2O3}}{I_{0Al2O3}} = \exp\left((-\mu\rho t)_{sample} - (-\mu\rho t)_{Al2O3}\right) \quad (2)$$

Assuming the Al_2O_3 tube and disk remain cylindrical shapes, the thickness (t) of the cylindrical sample or Al_2O_3 disk that the beam travels through is given as

$$t = 2\sqrt{r^2 - (x - x_0)^2} \quad (3)$$

where r is the radius of cylinder, x is the beam position along the scan direction, and x_0 is the center position of the cylinder. By substituting t in equation (2) with equation (3), the measured absorption profile becomes a function of the scan position x. We fitted ρ_{sample}, r and x_0 to minimize the standard deviation between the left side and right side of equation (2). ρ_{Al2O3} was calculated using its thermal equation of state [*Dubrovinsky et al.*, 1998]. μ_{Al2O3} was calculated from the mass attenuation of Al and O atoms at 40 keV [*Hubbell and Seltzer*, 1996]. μ_{sample} was estimated from the density of Fe-C alloy from a previous study, and corrected using the assumption that Ni incorporation changed the molecular mass without expanding the volume [*Jimbo and Cramb*, 1993]: this assumption was assumed to be independent of pressure and temperature for a fixed composition. The fitting uncertainty of ρ_{sample} was used as the uncertainty of sample density shown below. There might be additional uncertainties on estimating mass attenuation, calculating Al_2O_3 density, and possible misfits due to capsule deformation, which were estimated to cause 1-2% uncertainty on the final sample density.

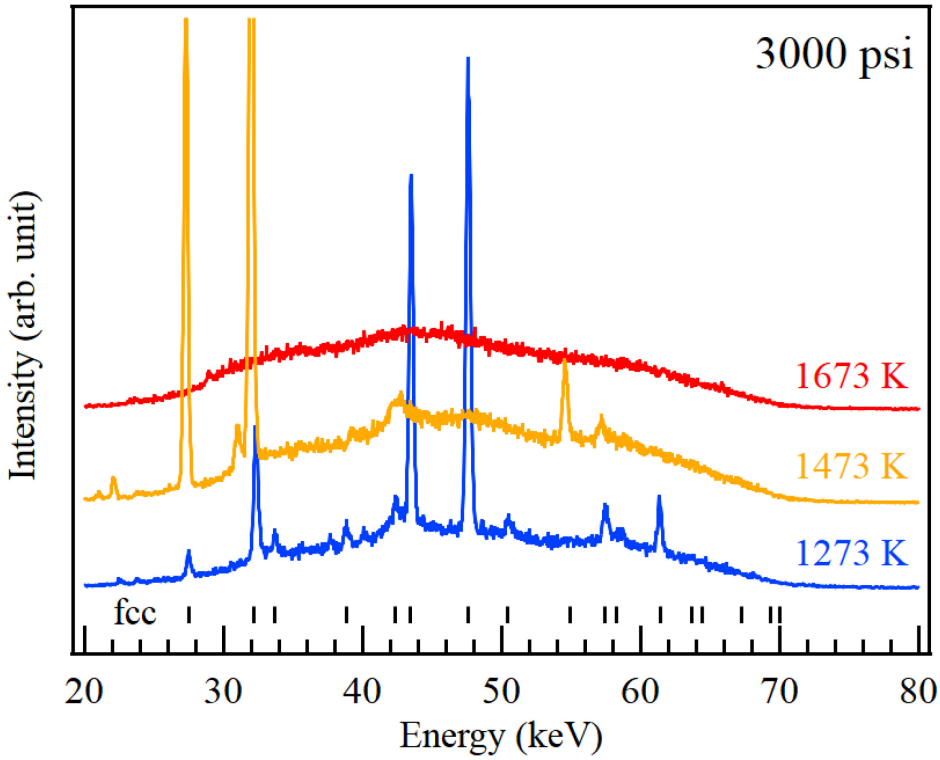

Figure 1. Representative energy-dispersive X-ray diffraction (EDXD) patterns of the FeNi-3C sample before and after melting under an oil load of 3000 psi. The patterns were collected at $2\theta = 20.1565^{o}$. The major peaks from the *fcc* (Fe,Ni) phase gradually disappeared upon heating from 1273 K to 1673 K. Graphite peaks are too weak to be identified, due to its low X-ray scattering factor. Fe_3C formation at subsolidus temperatures is slow and its main peaks are located below 20 keV. Partial melting at 1473 K results in the recrystallization of residual solid phase and the relative peak intensity variation.

2.2 First-principles molecular dynamics simulations

All the FPMD calculations were carried out based on a system of 192 atoms. For $Fe_{90}Ni_{10}$ with 5 wt% C, the computational system with 140 Fe +14 Ni + 38 C atoms was constructed by changing the composition of the Fe_3C structure, which was initially melted at 3000 K, and then the tempeteraure was reduced to the target temperatures at 1673 K and 1923 K, respectively. For $Fe_{90}Ni_{10}$ with 3 wt% C, the computational system containing 151 Fe + 17 Ni + 24 C atoms, was generated by modifying the composition of the 5 wt% C system. The computational supercells were scaled to different volumes for different pressure calculations. To understand the pressure and temperature effects on the structure and properties of the alloying liquids, the compositions and conditions were chosen as such for the convenience of comparing our results with previous data [*Lai et al.*, 2017; *Wang et al.*, 2019]. The averages based on the trajectories of the FPMD simulations were used to calculate the properties, such as the pressures and elasticity, of the liquids.

The FPMD modeling was based on Density Functional Theory (DFT) with plane wave basis sets as employed in the Vienna Ab initio Simulation Package (VASP) [*Kresse and Furthmüller*, 1996]. The Projector-Augmented Wave (PAW) method and exchange-correlation as parameterized by the Perdew–Burke-Ernzerhof (PBE) functional were applied in the Generalized Gradient Approximation (GGA) [*Blöchl*, 1994; *Perdew et al.*, 1992]. For Fe and Ni, 6d and 2s electrons (total of 8 electrons) and 8d and 2s electrons (total of 10 electrons) were treated as valence electrons, respectively, with their cores of [Ar] configurations. For C, 2p and 2s electrons (total of 4 electrons) were treated as valence electrons with its core of [He] configuration. The cut-off kinetic energy for the plane-wave basis was 520.00 eV and the Brillouin zone was sampled at the Γ point only. The initial electronic configuration was set to ferromagnetic but was allowed to change during the equilibration and equilibrium simulations.

The FPMD simulations were carried out with NVT and the Nosé-thermostat for up to 1 ps for the system to relax in the equilibration run for density calculations. The equilibration run was examined by monitoring parameters including the convergences such as force and energy, system stability, temperature, pressure, total energy fluctuation of the systems, the partition of the individual kinetic energy for each of the Fe, Ni and C subsystems, and the displacement of atoms. The time step was set to be 1 fs for all simulations. The total energy drift was calculated to be ~2–5 meV/atom/ps, suggesting good convergence and simulation stability. After the equilibration run, each of the FPMD simulations was run up to ~5 ps (5,000 steps) for statistical analysis of the density. The Pulay stress arising from the finite kinetic energy cutoff of the plane-wave basis set [*Francis and Payne*, 1990] and systematic errors from the GGA lead to an error in the computated pressure [*Perdew et al.*, 2008]. As a result, a correction of 3.77 GPa was applied to the calculated pressures based on the benchmark from the experimental density at ambient pressure from the previous data [*Jimbo and Cramb*, 1993; *Lai et al.*, 2017; *Wang et al.*, 2019]. The high pressure calculations were calibrated using experimental data on the density of iron at similar conditions.

3 Results

Experimental densities of Fe-Ni-C liquids were determined by fitting the X-ray absorption profiles at each *P-T* point. Figure 2a shows a set of representative absorption profiles of the FeNi-3C liquid at 5000 psi oil pressure (3-5.5 GPa) and continuously increasing temperatures. The height of the absorption peak correlates with the density of the sample. The abrupt change in the peak height from 1673 to 1873 K reflects the melting-induced density drop, where the melting temperature is consistent with the melting curve of the Fe-C system at ~5 GPa [*Fei and Brosh*, 2014].

Density of the sample, sample diameter, and its center position can be determined by fitting the absorption profile (see Figure 2b for a representative fitting). Densities of the FeNi-3C and FeNi-5C liquids as a function of pressure are plotted in Figure 3 (Table S1) along with data from previous studies. The results show that the density values of different studies are generally consistent within uncertainties. However, the compression trend shows significant scatter in all studies including the present work [*Sanloup et al.*, 2011; *Shimoyama et al.*, 2013; *Terasaki et al.*, 2010]. In these experiments, the scatter might result from several factors. First, the sample capsule can deform from the ideal cylindrical shape after the sample melts, which introduces uncertainty in the data fitting. Second, the temperature determination relies on the power curve, which contains about ±100 K uncertainty. Third, the temperature uncertainties also influenced

the pressure calibration through the thermal equation of states of MgO and Pt: this effect involves an error of ~0.8 GPa / 100 K at most.

The compression data of the FeNi-3C and FeNi-5C liquids were fitted by the Birch-Murnaghan equation of state (EoS). Table 1 lists the results of the density and elasticity of liquid Fe-(Ni)-C obtained from this study as well as those from previous works. The densities of FeNi-3C and FeNi-5C liquids in this study and Fe-(Ni)-C alloys with 3-7 wt% C from previous studies are ~2-3.6% lower than that of the pure Fe or Fe-Ni at the same temperatures and this decrement is consistent over the pressure range [*Anderson and Ahrens*, 1994] (Figure 3). However, fitting the bulk moduli from the scattered ρ–P data shows contradicting results between different studies. In this study, the fitting yields ρ_0 = 6.86 g/cm^3, K_{T0} = 99(13) GPa, K_{T0}'=4 (fixed) for the FeNi-3C liquid at ~1923 K, and ρ_0 = 6.77g/cm^3, K_{T0} = 97(12) GPa, K_{T0}'=4 (fixed) for the FeNi-5C liquid at ~1823 K. The ρ_0 has an uncertainty level of 0.5-0.7% in the EoS fitting itself, but this was then fixed to the ambient value by applying a normalization to all obtained ambient pressure densities [*Jimbo and Cramb*, 1993]. If K_{T0}' is fixed at 5.5 or 7.0 in accord with the theoretical calculations shown below, K_{T0} decreases to 90(13)/83(13) GPa and 90(12)/84(12) GPa for FeNi-3C and FeNi-5C, respectively. Confidence ellipses showing the correlation between K_{T0} and K_{T0}' are presented in Figure S2. A recent study suggested that the Murnaghan EoS has better data reproducibility of Fe liquid when extrapolating to pressures greater than 100 GPa [*Nakajima et al.*, 2015]. We also use the Murnaghan EoS to fit the data, and the results show little difference from the Birch-Murnaghan EoS. Our determined bulk moduli of FeNi-3C and FeNi-5C are thus slightly higher than that of pure Fe, which gives K_{T0} = 85.1 GPa with K_{T0}'=4.66 [*Anderson and Ahrens*, 1994]. This is in contrast with those in some previous density studies, in which Fe-C liquids were characterized as significantly softer than pure Fe [*Shimoyama et al.*, 2013; *Terasaki et al.*, 2010], but consistent with the results from the sound velocity measurements [*Kuwabara et al.*, 2016; *Nakajima et al.*, 2015; *Shimoyama et al.*, 2016] and a previous theoretical calculation [*Belashchenko et al.*, 2011]. The reasons for the discrepancies in bulk moduli K_{T0} are attributed to the small pressure range, limited data points and large uncertainties in density measurements.

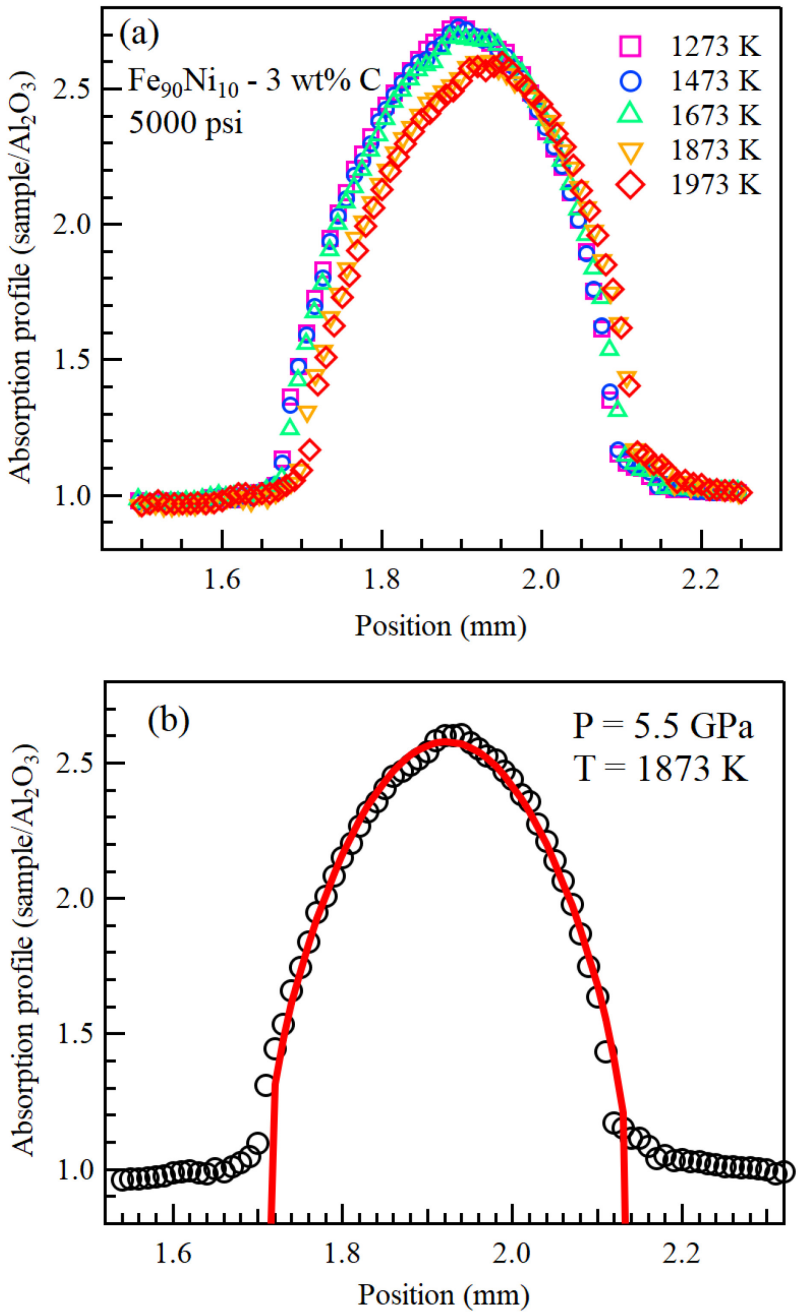

Figure 2. Representative X-ray absorption profiles of the Fe-Ni-C liquids. (a) X-ray absorption profiles of FeNi-3C at 5000 psi oil pressure and 1273-1973 K. The depression of peak height between 1673 K and 1873 K correlates to the density drop caused by the full melting of the sample; (b) Fitting of FeNi-3C absorption profile at 8.4 GPa and 2073 K by the Beer-Lambert law.

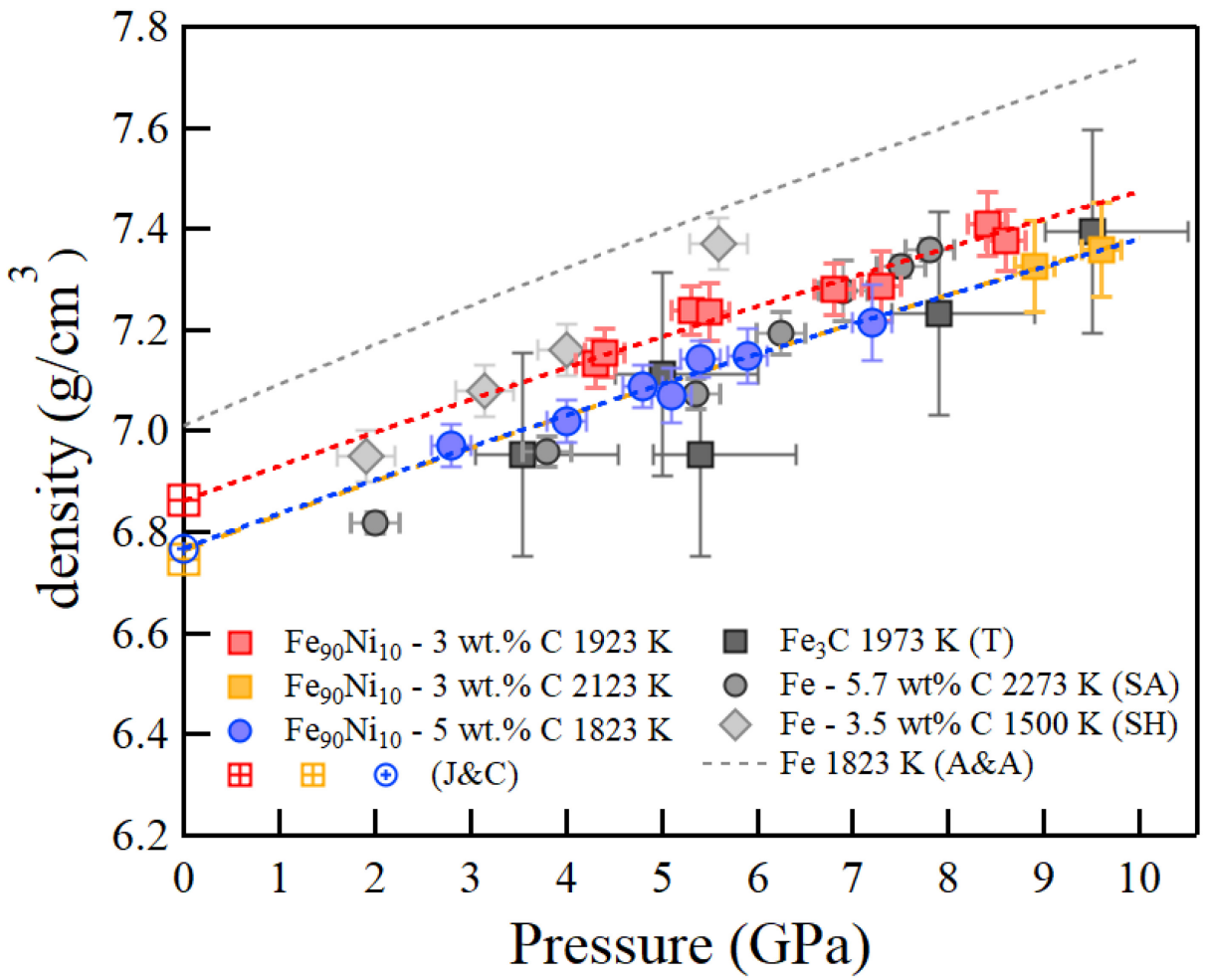

Figure 3. Density of Fe, Fe-C and Fe-Ni-C liquid as a function of pressure. The red and orange curve shows the EoS of FeNi-3C at ~1923(±50) K and ~2123(±50) K, respectively. The blue curve shows the EoS of FeNi-5C at ~1823(±50) K. The density of Fe at the same temperature was plotted for reference, and the density of $Fe_{90}Ni_{10}$ would be 0.5% higher than pure Fe assuming Ni-Fe substitution influences only the molecular weight without changing the molecular volume. Data sources: J & C - *Jimbo and Cramb* [1993], T - *Terasaki et al.* [2010], SA - *Sanloup et al.* [2011], SH - *Shimoyama et al.* [2013] and A&A - *Anderson and Ahrens* [1994].

290 **Table 1. EoS parameters of Fe-(Ni) and Fe-(Ni)-C liquid alloys.**

Composition	ρ_0 (g/cm3)	T_0 (K)	K_{T0} (GPa)	K_{S0} (GPa)	K_0'	Reference
			Fe-(Ni)			
Fe	7.019	1811	85.1*	109.7(7)	4.66(4)	[*Anderson and Ahrens*, 1994]
Fe	6.91	1673		105(2)	6.7(10)	[*Jing et al.*, 2014]
Fe	7.014	1820	62		-	[*Belashchenko et al.*, 2011]
$Fe_{90}Ni_{10}$	6.97	1799-2183		103(2)	5.7(8)	[*Kuwabara et al.*, 2016]
Fe-(Ni)-C						
$Fe_{90}Ni_{10}$-3 wt%C	6.86	1923	99(13)	123*	4	this study (experiment)
			90(13)	112*	5.5	
			83(13)	103*	7	
	6.77	1823	97(12)	119*	4	this study (experiment)
$Fe_{90}Ni_{10}$-5 wt%C			90(12)	111*	5.5	
			84(12)	104*	7	
$Fe_{90}Ni_{10}$-3 wt%C	6.93(4)	1673	72(6)†		5.9(5)	this study (FPMD-GGA)
	6.84(2)	1923	72(4)†		5.4(3)	
	-	4050	75(9)		6.4(3)	
$Fe_{90}Ni_{10}$-5 wt%C	6.91(2)	1673	89(3)†		5.4(2)	this study (FPMD-GGA)
	6.79(1)	1923	84(2)†		5.1(2)	
	-	4050	78(4)		6.4	
Fe_3C (Fe-6.7wt%C)	6.46	1973	50(7)		4-7	[*Terasaki et al.*, 2010]
Fe-3.5wt%C	7.012	1500	55.3(25)		5.2(15)	[*Shimoyama et al.*, 2013]
Fe-3.5wt%C	6.91	1700	83.9	100(1)	5.9(2)	[*Shimoyama et al.*, 2016]
Fe-3.9wt%C		1500	100			[*Nakajima et al.*, 2015]
	6.505	2500	82	110(9)	5.14(30)	

Fe-3.5wt%C	6.657	1600	97.3		-	[*Belashchenko et al.*, 2011] (MD)
$Fe_{90}Ni_{10}$-4 wt%C	6.82	1799-2183		110(2)	7.6(6)	[*Kuwabara et al.*, 2016]

*K_{T0} and K_{S0} are converted through $K_{S0} = K_{T0}(1+\alpha\gamma T)$, in which α is the thermal expansion and γ is the Gruneisen parameter (fixed at 1.735 for pure Fe).
†GGA calculations may systematically underestimate the density and bulk modulus.

We performed FPMD calculations on FeNi-3C and FeNi-5C liquids at the same temperature range and over a wider pressure range to complement our experimental results (Figure 4a and Table 1). The calculated densities of FeNi-3C and FeNi-5C liquids were benchmarked using the densities from experiments at ambient pressure [*Jimbo and Cramb*, 1993]. We found that K_{T0} obtained from calculated data are ~6-18 GPa lower than the experimental results, while the K_{T0}' values fall within a range of 5.1-5.9, and clearly are consistently higher than 4 (Table 1). We thus performed fits to our experimental data by fixing K_{T0}' to 5.5 for comparison and extrapolation (Table 1). The slightly lower calculated K_{T0} values relative to experiments is consistent with the typical underestimation of K_{T0} by the GGA method. Our calculated K_{T0} for Fe-Ni-C liquids are still similar to those of liquid Fe [*Anderson and Ahrens*, 1994], but significantly higher in comparison with the K_{T0} values from previous density measurements [*Shimoyama et al.*, 2013; *Terasaki et al.*, 2010]. In the calculations, the FeNi-5C liquid appear to have a higher K_{T0} than the FeNi-3C liquid, suggesting that adding carbon may increase the incompressibility of Fe-Ni-C liquids. This is consistent with the trend from Fe to Fe-Ni-C in the experiments [*Anderson and Ahrens*, 1994; *Kuwabara et al.*, 2016], although experiments do not have the resolution to distinguish an elastic difference between FeNi-3C and FeNi-5C. The bulk modulus has a weakly negative temperature dependence in the calculations, resulting in the density difference from 1673 K to 1923 K shrinking as pressure increases (Figure 4). This indicates the thermal expansion decreases with pressure in Fe-Ni-C liquids, which is in accord with typical systematics of thermal expansion under compression (e.g., *Duffy and Ahrens,* 1993).

We also performed four additional sets of FPMD calculations to the pressure range of Earth's core, and at much higher temperatures of 4050 K and 5530 K (as also apropos to Earth's core). These calculations gave a higher $K_{T0}' = 6.4$ compared with the lower pressure calculation, which corresponds to about $K_{T0}' = 7$ at ~1900 K (Figure 4b, Table 1). The fits, when back-extrapolated to the low pressure range, are not completely consistent with the low-temperature calculations. This mismatch might be indicative of structural changes occurring within the liquid between the lower and higher pressure/temperature regimes: indications of such structural changes have been derived from past molecular dynamics simulations (e.g., *Wang et al.,* 2019). The higher pressure simulations certainly yield a better constraint on K_{T0}' at the core conditions for density and sound velocity extrapolation. Considering the effect of temperature on the bulk modulus, the Fe-Ni-C alloys still have a higher K_0 than pure Fe within these simulations: as such the modest stiffening of the C-bearing alloys relative to Fe appears to be a robust result.

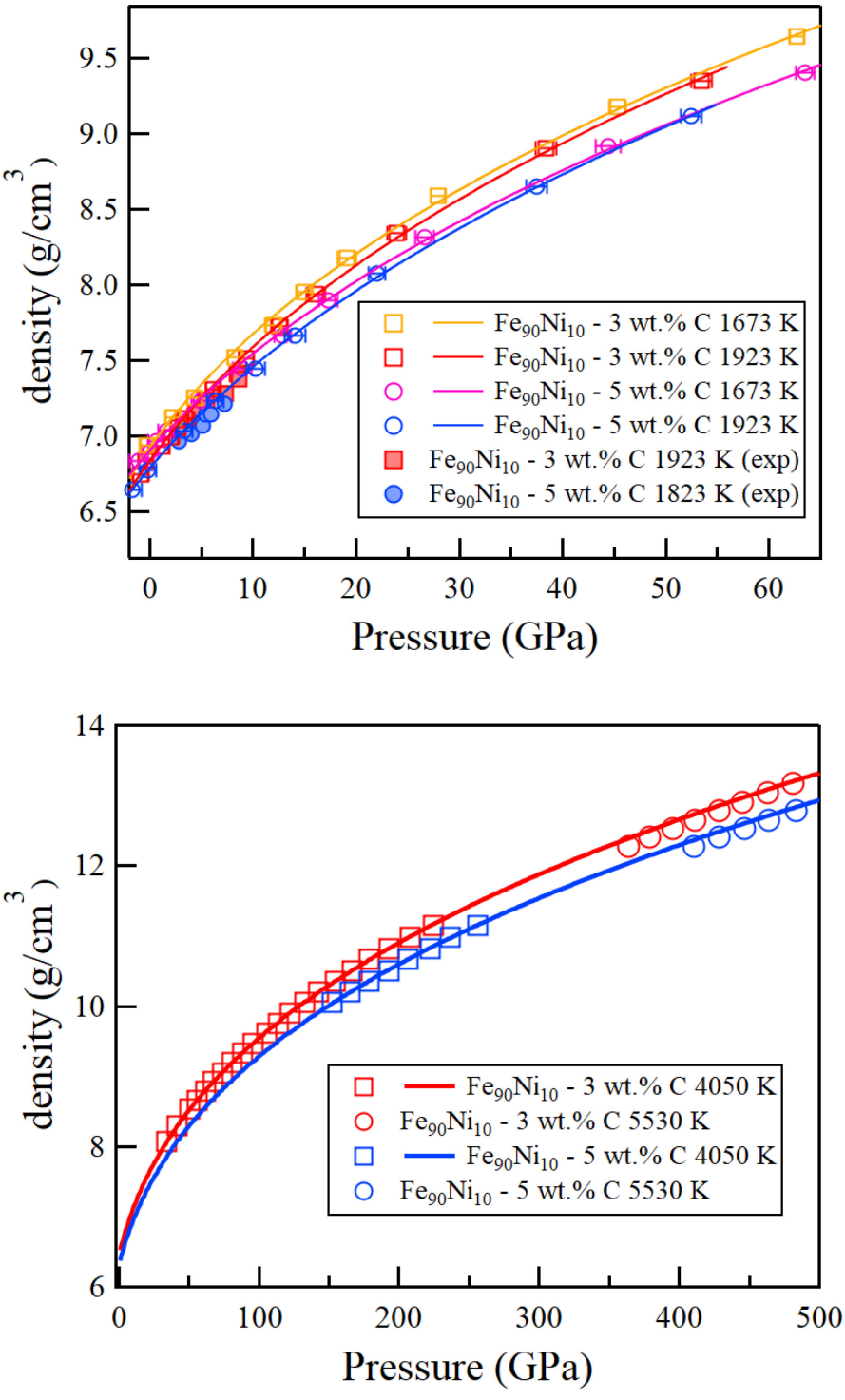

Figure 4. Density of FeNi-3C and FeNi-5C as a function of pressure obtained from FPMD calculations (a) at 1673 and 1923 K up to ~65 GPa & (b) at 4050 and 5530 K up to core pressures. The curves show the 3rd-order Birch-Murnaghan equations of states fits. The uncertainties of pressures are mostly within the symbol size. The solid symbols show the experimental data for comparison.

We further calculated compressional sound velocities, v_p, from the densities and bulk moduli in order to assess the reliability of the estimates of the liquid bulk moduli by comparing them with the better constrained ambient pressure v_p measurements.

$$v_p = \sqrt{K_s/\rho} \quad (4)$$

where

$$K_S = K_T(1 + \alpha\gamma T) \quad (5)$$

We also calculated the thermal expansion as α=0.73×10^{-4} K^{-1} from the experimental data of FeNi-3C from 1923(50) K to 2123(50) K in this study. We found it to be consistent with the two estimates, 0.76-0.86×10^{-4} K^{-1} and 0.86×10^{-4} K^{-1} for Fe-3.5 wt.%C [*Jimbo and Cramb*, 1993; *Shimoyama et al.*, 2013]. The Grüneisen parameter γ was fixed at 1.735 for pure Fe [*Anderson and Ahrens*, 1994]. We tested the γ with a ±0.2 deviation and the v_p shows little change associated with this deviation (Fig. S3). We compare the v_p calculated from experimental studies in Figure 5. The v_p range of 3.8-4.2 km/s was marked as a reference range from the sound velocity measurement at ambient pressure at ~1600-2000 K (*Pronin et al.,* 1964). Those v_p values corresponding to K_{S0} similar to or higher than pure Fe match well with the ambient measurement, while the v_p values derived from low K_{S0} values are significantly lower. This indicates that previous density measurements might largely underestimate the bulk moduli of Fe-(Ni)-C alloys [*Shimoyama et al.*, 2013; *Terasaki et al.*, 2010]. The bulk moduli determined from our density measurements with denser data coverage agree reasonably well with the sound velocity measurements [*Kuwabara et al.*, 2016; *Nakajima et al.*, 2015; *Shimoyama et al.*, 2016].

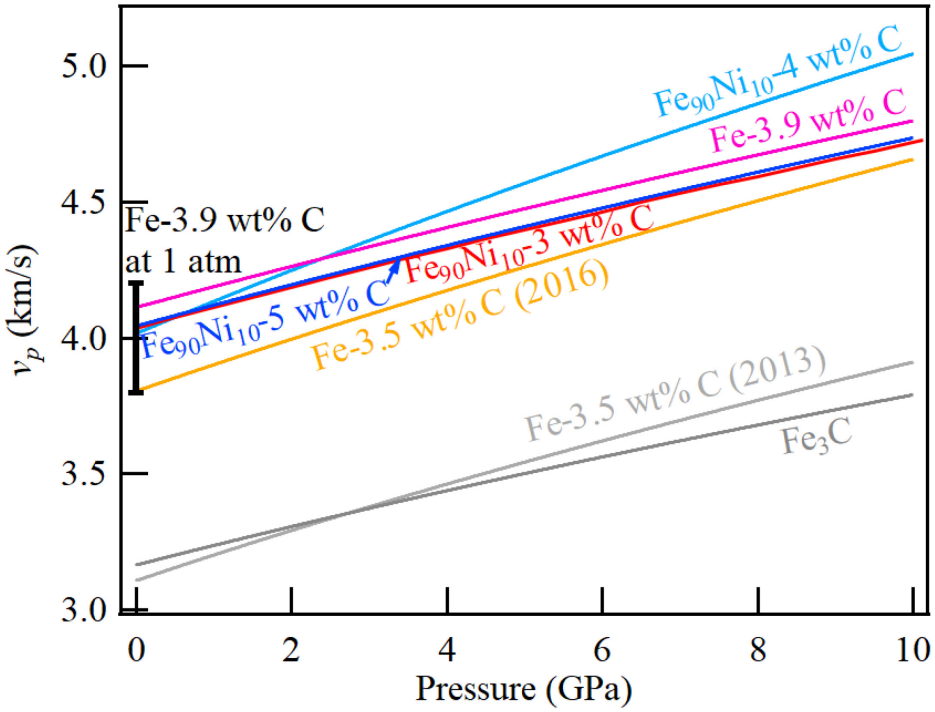

Figure 5. v_p of Fe-(Ni)-C liquids calculated from bulk modulus and density. The EoS parameters and references can be found in Table 1, referenced to chemistries (in most instances) or dates. The current study's results are shown in red and dark blue. The black bar at 0 GPa covers the v_p range of Fe-3.5 wt% C from ~1600 K to ~2000 K at ambient pressure as obtained by ultrasonic measurements [*Pronin et al.*, 1964].

4 Discussion

4.1 Effect of K' on the v_p of liquid Fe alloys and carbon in Earth's core

Our experiments and calculations suggest that the alloying of carbon increases the bulk modulus and thus v_p of liquid Fe, contrary to previous density measurements [*Shimoyama et al.*, 2013; *Terasaki et al.*, 2010]. Therefore, the prior arguments that disfavored carbon as the light element in the outer core need to be reassessed, as these were based on previous low estimated values of the bulk modulus and v_p of Fe-C liquids [*Terasaki et al.*, 2010]. As importantly, the extrapolated ratio of K(Fe-alloy)/K(Fe) at core pressures can significantly differ from K_0(Fe-alloy)/K_0(Fe) at ambient pressure, because the increment of K derived from the $K'P$ term largely diminishes the contribution of K_0. In short, the bulk modulus of iron-rich core alloys at core conditions are largely modulated by K', rather than K_0, and a relatively small difference in K_0' can lead to a significant difference in K and thus v_p at core pressures. However, K_0' values of the liquids are usually poorly constrained due to the limited pressure range and sparse data coverage in experiments on liquids. For instance, our compression data at <10 GPa can be reasonably fit using the Birch-Murnaghan / Murnaghan EoS by fixing K_0' at 4, 5.5 or 7; however, using a K_0'=5.5 or 7 for extrapolation can result in significantly different K and v_p values along the adiabatic P-T conditions of the liquid outer core (Figure 6a). If the inner core boundary (ICB) temperature is fixed at 5000 K, the difference in v_p between fixing K_0'=5.5 and 7 is about –0.59 km/s at 0 GPa, due to the difference in temperature and K_0, but reverses to ~1 km/s near core mantle boundary (CMB), and reaches ~1.8 km/s at the inner-core boundary (ICB). This reversal is essentially entirely controlled by the difference in K'. We tried to tune the ICB temperature from 5000 to 6000 K, and found the v_p deviation is <0.1%. Thus, the uncertainty in fitting K' introduces major challenges in quantifying the light element in the outer core during data extrapolation.

Existing experimental data on liquid iron-alloy densities are scattered and, with the exception of sparse shock Hugoniot data that access the liquid field at extreme pressure and temperature conditions, are limited to only pressures below 10 GPa. Therefore, K_0' is typically fixed to 4 or 4.66 of liquid Fe in EoS fitting in most of these studies (4.66 is the default value arrived at by *Anderson and Ahrens,* 1994). Our DFT calculations over a larger pressure range provide a more realistic constraint on K_0', although systematic errors may be introduced by the approximations adopted in the calculation. If we use K_0'=7.0 for the FeNi-3C and FeNi-5C liquids, and assume a linear relation between the sound velocity and the carbon content, the carbon content in the outer core is estimated at 0.45 wt% (mixing Fe and FeNi-3C) or 0.75 wt% (mixing Fe and FeNi-5C) in order to match the PREM model at CMB conditions, which is slightly lower than the previous estimate at 1.2–0.9 wt% from a sound velocity measurement [*Nakajima et al.*, 2015]. On the other hand, the carbon required to match the density is higher, ~1.7–2.5 wt% at CMB conditions (Figure 6b). Nakajima et al. [2015] suggested that the Earth's outer core is carbon-depleted with <1.2 wt% C, based on the difficulty of carbon as the sole light element to match both the sound velocity and density of Earth's outer core. Since the outer core

could contain more than one light element, we would argue that a carbon content higher than 1.2 wt% may not be ruled out as the primary light element in the core, if the outer core contains another light element which lowers both ρ and v_p of Fe. In this case, the carbon content will be lower than 1.7-2.5 wt% if the ρ and v_p of the mixture follow a linear extrapolation. A key feature of our new data is that small weight percentages of carbon are highly efficient at both increasing the sound velocity and decreasing the density of iron: the effect of carbon on the elasticity of liquid iron alloys is augmented relative to prior studies [e.g., *Nakajima et al.,* 2015]. This marked effect of carbon is likely produced by its low atomic number and hence comparatively high molar content at low weight percentages. These molar mass abundance effects are particularly notable for carbon because of its generation of highly incompressible Fe/Ni-C bonds within the alloy (e.g., *Wang et al.,* 2019). Indeed, while 1-2% carbon may be present in the outer core, it remains quite possible that if smaller quantities of carbon are present, the notable elastic effects of carbon could markedly shift the amount of other lighter alloying elements in the core required to generate the core density-sound velocity trends. This conclusion is in general accord with past theoretically based inversions of core composition [*Badro et al.,* 2014].

Notably, K_0' becomes dominant in determining the slope of the v_P-P curve, given the increased effect of K_0' on the v_p calculation at high pressures. In an adiabatic Murnaghan EoS,

$$K_S = K_{S0} + K_S' P \quad (6)$$

and

$$\rho = \rho_0 \left(1 + \frac{K_S'}{K_{S0}} P\right)^{\frac{1}{K_S'}} \quad (7)$$

thus

$$v_p = \sqrt{\frac{K_S}{\rho}} = \sqrt{\frac{K_{S0}}{\rho_0}} \left(1 + \frac{K_S'}{K_{S0}} P\right)^{\frac{1}{2} - \frac{1}{2K_S'}} \quad (8)$$

its pressure derivative

$$\frac{dv_p}{dP} = \frac{1}{2}(K_S' - 1) \sqrt{\frac{1}{\rho_0 K_{S0} \left(1 + \frac{K_S'}{K_{S0}} P\right)^{1 + \frac{1}{K_S'}}}} = \frac{1}{2}(K_S' - 1) \sqrt{\frac{1}{\rho K_S}} \quad (9)$$

In addition to (K_S'-1), K_S' will also have much larger influence on K_S and ρ terms compared with K_{S0} at elevated pressures, which makes K_S' a dominant factor in determining the slope of v_p from the CMB to the ICB. Liquid Fe with K_0'=4.66 from a shockwave EoS [*Anderson and Ahrens*, 1994] has a slope very close to the seismic PREM model, and thus the Fe-light element alloy in the outer core may need a K_0' close to that of PREM with a higher v_p at ambient pressure to match both the slope and value of v_p in the PREM model. While carbon can increase v_p at ambient pressure, the K_0' values of 5.5 or 7 in an adiabatic Murnaghan EoS appear to be too high to match the v_p of CMB and ICB simultaneously (Fig. 6a). Note that the two types of EoSs do not yield consistent elastic values, resulting in the adiabatic Murnaghan EoS requiring a K_0' of ~3.7 instead of ~4.6 to match the PREM slope. Again, this indicates tbat carbon cannot be the

437 only dominant light element in the outer core. If carbon plays the role to elevate the v_p of the
438 core, one or more light elements are needed to soften the Fe alloy to match the slope of PREM
439 over the outer core pressure range.

440

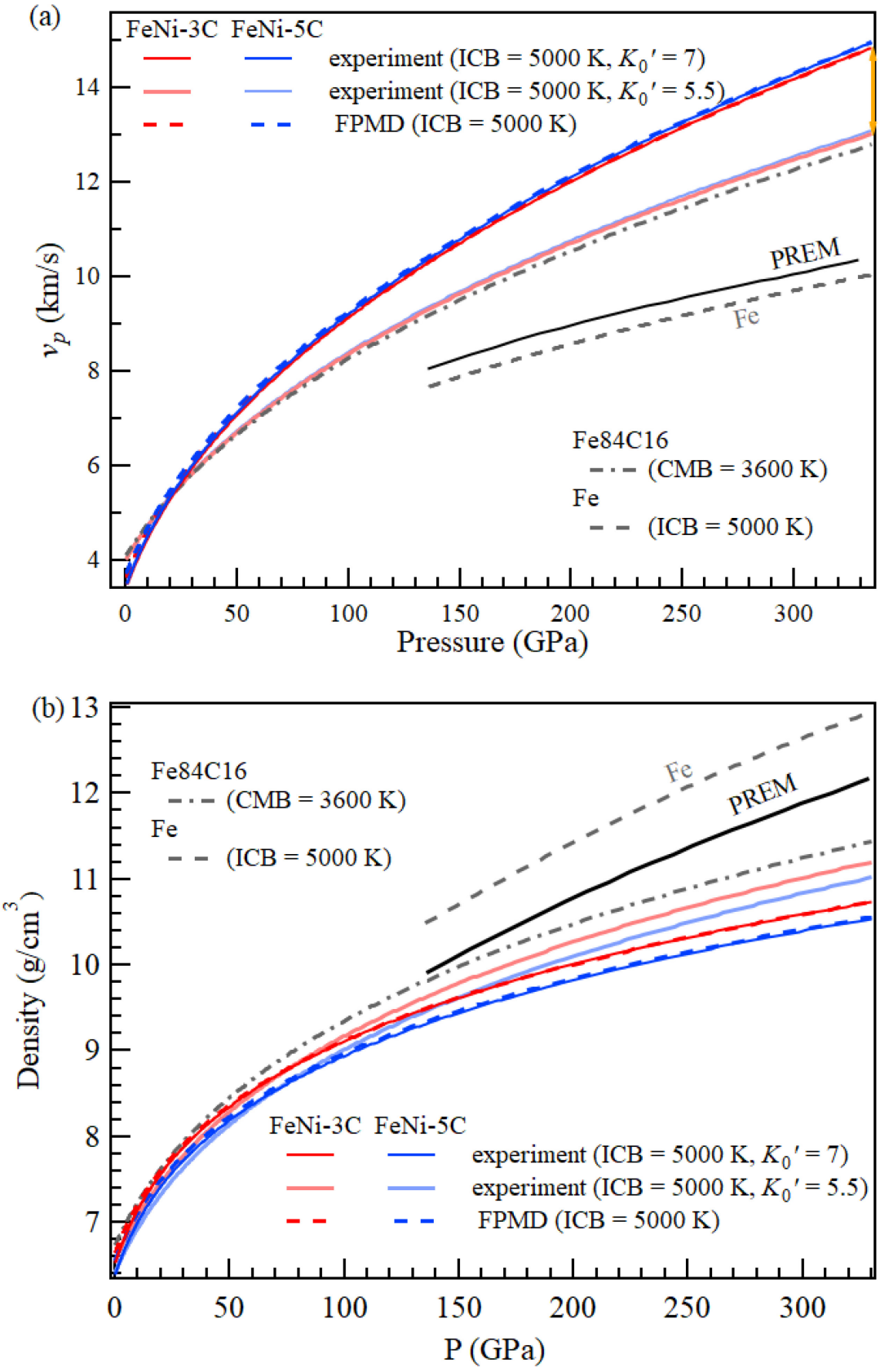
(a)
FeNi-3C FeNi-5C
experiment (ICB = 5000 K, K_0' = 7)
experiment (ICB = 5000 K, K_0' = 5.5)
FPMD (ICB = 5000 K)
PREM
Fe
Fe84C16
(CMB = 3600 K)
Fe
(ICB = 5000 K)
v_p (km/s)
Pressure (GPa)
(b)
Fe84C16
(CMB = 3600 K)
Fe
(ICB = 5000 K)
Fe
PREM
FeNi-3C FeNi-5C
experiment (ICB = 5000 K, K_0' = 7)
experiment (ICB = 5000 K, K_0' = 5.5)
FPMD (ICB = 5000 K)
Density (g/cm^3)
P (GPa)

441

Figure 6. Extrapolation of v_p and density of FeNi-3C and FeNi-5C to Earth's outer core conditions along isentropes. (a) Calculated v_p to outer core conditions. Inner core boundary (ICB) temperatures of 5000 K at 330 GPa were considered as the anchor point. The v_p deviations from a 2 wt% C compositional variation are <0.12 km/s in the entire outer core *P-T* range (red/blue solid/dashed lines). The deviation caused by changing K_0' from 5.5 to 7 at 1923/1823 K in the EoS fitting results in a large v_p deviation of ~1.9 km/s at ICB conditions (orange double arrows), which shows that the K' difference induces a major deviation during data extrapolation. (b) Calculated density to outer core conditions. The experimental and simulated results are both anchored at an ICB temperature of 5000 K, corresponding to the velocity curve in (a). The black, grey dashed and grey dotted dashed lines show the PREM reference [*Dziewonski and Anderson*, 1981] and previous results on Fe [*Anderson and Ahrens*, 1994] and $Fe_{84}C_{16}$ [*Nakajima et al.*, 2015] for comparison. Temperature dependences of K_0, K' and α of Fe-Ni-C liquid are from previous density and sound velocity measurements [*Nakajima et al.*, 2015; *Ogino et al.*, 1984].

While the adiabatic Murnaghan EoS has been widely applied in the study of liquid density and sound velocity [*Jing et al.*, 2014; *Kawaguchi et al.*, 2017; *Nakajima et al.*, 2015], it should be noted that the absence of 2nd and higher pressure derivatives within this simple EoS likely results in the overestimation of v_p at extremely high pressure and lead to some unreasonable results. For example, when a liquid adopts a higher K_0' than its corresponding solid phase, which is usually the case since materials with a positive Clapeyron slope on melting have a lower density and likely more compressible liquid, the v_p of the liquid could ultimately intersect the bulk sound velocity of the solid (which neglects, of course, the shear modulus). The v_p of Fe-Ni-C liquid in this and previous studies both become higher than the bulk sound velocity of Fe_3C at ~140-220 GPa [*Chen et al.*, 2018; *Nakajima et al.*, 2015], indicating that higher-order pressure derivatives of the bulk modulus are likely essential to properly calculate the v_p above this pressure. The v_p extrapolation, especially above CMB pressurse, might thus be overestimated (Fig. 6a), which in turn would underestimate the carbon content needed to match the v_p in PREM model.

Our measurements indicate that incorporation of carbon in liquid Fe lowers its density, but the Fe-Ni-C liquids have similar or slightly higher bulk modulus compared to liquid Fe, which leads to higher v_p than Fe liquid. Therefore, carbon may still account for a portion of the seismic observations of Earth's outer core, as might other light elements like S and Si [*Kawaguchi et al.*, 2017; *Terasaki et al.*, 2019]. It also agrees with a recent FPMD simulation, in which all light elements including O, Si, S and C were shown to elevate the v_p of Fe at CMB to ICB conditions [*Badro et al.*, 2014]. However, from the very similar K_S values ($= \rho v_p^2$) for all different Fe-light element alloys at the same pressure, we inferred the K_0' in the Birch-Murnaghan EoS fittings were fixed or narrowly constrained, resulting in the calculated v_p being roughly proportional to $\rho^{-1/2}$ at core pressures while ρ decreases linearly with light element concentration. This similar K' of all Fe-light element alloy is not consistent with our FPMD calculations that start from 0 GPa, but might be reasonable when the pressure is extremely high which may make the compressibility of all alloy liquids approach those of closely-packed Fe. Giving the dominant influence K' has on calculating $v_p$under core conditions, further study might still be needed to testify the adopted EoS and K_0' treatment in our and previous FPMD calculations. Overall, giving the uncertainties from the numerical fittings and effects from other light elements, the effect of carbon is clear. Both experimental results and computer simulations

suggest that carbon effectively reduces the density while it increases the v_p of Fe-Ni alloy, which may qualitatively account for a portion of the seismic observations of Earth's outer core.

4.2 Carbon in the lunar outer core

Carbon has also been suggested as the dominant light element in the lunar outer core [*Steenstra et al.*, 2017]. Since the pressure range of the lunar core was experimentally reached in the present study, our experimental results can be directly used to understand the role of carbon in the lunar outer core. It is noteworthy that the size and density of lunar core have not been well constrained, and that the current estimates of the size and density at 380 km and 5.1 g/cm^3, or 250-290 km and 6.5 g/cm^3 were based on the assumption that S is the dominant light element component [*Garcia et al.*, 2012; *Jing et al.*, 2014]. Therefore, the density of Fe-(Ni)-C liquid cannot be directly compared to these estimates due to the S-rich assumption. Instead, the v_p calculated from the obtained density and bulk modulus can be compared directly with inversions of the Apollo seismic data [*Weber et al.*, 2011]. We plotted the v_p of Fe alloys as a function of pressure in Figure 7 with the current estimated v_p range at ~5.2 GPa in the lunar core model. The pressure interval of the lunar core is fixed to a single pressure due to its small size. The estimated lunar core v_p at 4.1 km/s [*Weber et al.*, 2011] is slightly lower than that of pure $Fe_{90}Ni_{10}$, and thus any light element needs to lower the v_p of pure Fe-Ni alloy. At a temperature near the melting point of Fe-Ni-C alloy, the incorporation of 3-5 wt.% carbon both increases the v_p of pure Fe-Ni alloy around 5.2 GPa. This result, based on the core v_p estimate, suggests that Fe-Ni-C liquid does not match well with the v_p of lunar outer core. The same problem applies to Fe-Si [*Terasaki et al.*, 2019; *Williams et al.*, 2015]. However, the Fe-S liquid reduces the v_p at low pressure, which can better match with the anchored cross point of pressure and v_p [*Jing et al.*, 2014; *Terasaki et al.*, 2019]. The uncertainty of the only seismic data, however, can be significant and the possibility that the v_p is 4.3 km/s or higher cannot be ruled out, which would make the incorporation of carbon potentially plausible. Nevertheless, based on the available data and current seismic velocity estimate for the lunar core, we suggest that the incorporation of carbon as major light element in lunar outer core is less possible with the current v_p estimation, but further seismic constraints are still needed to constrain the light element specie(s).

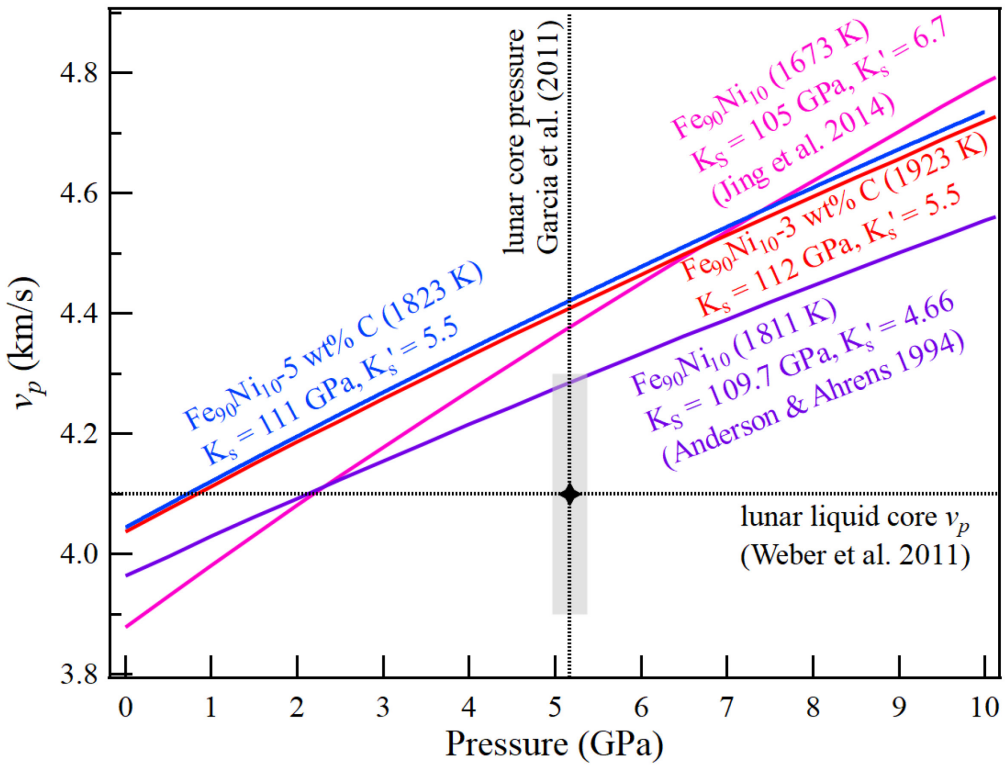

Figure 7. Compressional sound velocity v_p of $Fe_{90}Ni_{10}$, FeNi-3C and FeNi-5C in comparison with lunar core model. The vertical and horizontal gray dashed lines mark the estimated lunar core pressure and v_p, which cross at 5.2 GPa and 4.1 km/s. The shaded area around shows the potential uncertainty for these two estimations. The EoS of $Fe_{90}Ni_{10}$ used the data of pure Fe with a density correction taking into account the change in molecular weight.

5 Conclusions

We have carried out density measurements on Fe-Ni-C liquids and demonstrated that carbon incorporation lowers the density of liquid Fe-Ni alloys with slightly increases or minimal changes in the bulk moduli, leading to a higher compressional sound velocity than Fe-Ni liquids. At present, a precise determination of the species and amount of light elements in Earth's outer core is difficult due to the large uncertainty inherited from the uncertainty in K' during data extrapolation and potentially complex coupling among multiple light elements. This uncertainty is significantly larger on v_p than on the density, thus matching the density is possibly a more useful way to estimate the content of light element when extrapolating from low pressure. Increasing the measurable pressure range of liquid density can significantly improve the error of K' determination, which is needed for studying planetary liquid cores. In this sense, well-benchmarked computational approaches such as first-principles molecular dynamics can complement experimental investigations.

The effect on sound velocity by incorporating C from the present study is in contrast with the results from some previous experimental measurements on density, but consistent with the results on sound velocity based on ultrasonic, inelastic X-ray scattering measurements and theoretical calculations. The tendency of carbon to increase the v_p of Fe makes it a strong

candidate light element in Earth's outer core with higher v_p than liquid Fe. Carbon may not be a major light element in the lunar outer core and other terrestrial bodies with low v_p in their liquid cores. The different trend in seismically determined v_p compared with Fe-Ni liquids may indicate different major light elements in the liquid cores of Earth and Moon, which is a potential result from the distinct partition behavior of siderophile elements under different pressure-temperature conditions [*Dasgupta et al.*, 2013], or from the extent that carbon is crystallized and concentrated in the solid inner core [*Wood*, 1993].

Acknowledgments, Samples, and Data

Experiments used resources of the Advanced Photon Source, a U.S. Department of Energy (DOE) Office of Science User Facility operated for the DOE Office of Science by Argonne National Laboratory under Contract No. DE-AC02-06CH11357. X-ray absorption experiments were performed at HPCAT (Sector 16), Advanced Photon Source (APS), Argonne National Laboratory. HPCAT operations are supported by DOE-NNSA's Office of Experimental Sciences. This experimental work was supported by NSF grants (EAR-1555388, EAR-1565708, EAR-1829273) to BC. The computational work was supported by NSF grant (EAR-1565678) to JW. X. Lai was supported by National Natural Science Foundation of China grant (no. 42002041). Y. Kono acknowledges support by JSPS KAKEN- HI grant (19KK0093). Q. Williams was supported by NSF EAR-2017294. This research used resources of the National Energy Research Scientific Computing Center, a DOE Office of Science User Facility supported by the Office of Science of the U.S. Department of Energy under Contract No. DE-AC02-05CH11231. Portions of this research were conducted with high performance computing resources provided by Louisiana State University (http://www.hpc.lsu.edu). All the data necessary to produce the results are present in the manuscript and supplements for review purposes, and will be available on Zenodo by acceptance.

562 **References**

563 Anderson, W. W., and T. J. Ahrens (1994), An equation of state for liquid iron and implications
564 for the Earth's core, *Journal of Geophysical Research: Solid Earth*, *99*(B3), 4273-4284.

565 Badro, J., A. S. Côté, and J. P. Brodholt (2014), A seismologically consistent compositional
566 model of Earth's core, *Proceedings of the National Academy of Sciences*, *111*(21), 7542-
567 7545.

568 Belashchenko, D. K., A. Mirzoev, and O. Ostrovski (2011), Molecular dynamics modelling of
569 liquid Fe-C alloys, *High Temperature Materials and Processes*, *30*(4-5), 297-303.

570 Birch, F. (1952), Elasticity and constitution of the Earth's interior, *Journal of Geophysical*
571 *Research*, *57*(2), 227-286.

572 Blöchl, P. E. (1994), Projector augmented-wave method, *Physical review B*, *50*(24), 17953.

573 Brett, R. (1971), The earth's core: Speculations on its chemical equilibrium with the mantle,
574 *Geochimica et Cosmochimica Acta*, *35*(2), 203-221.

575 Chen, B., J. Li, and S. A. Hauck (2008), Non-ideal liquidus curve in the Fe-S system and
576 Mercury's snowing core, *Geophysical Research Letters*, *35*(7).

577 Chen, B., L. Gao, B. Lavina, P. Dera, E. E. Alp, J. Zhao, and J. Li (2012), Magneto-elastic
578 coupling in compressed Fe7C3 supports carbon in Earth's inner core, *Geophysical*
579 *Research Letters*, *39*(18).

580 Chen, B., X. Lai, J. Li, J. Liu, J. Zhao, W. Bi, E. E. Alp, M. Y. Hu, and Y. Xiao (2018),
581 Experimental constraints on the sound velocities of cementite Fe_3C to core pressures,
582 *Earth and Planetary Science Letters*, *494*, 164-171.

583 Chen, B., Z. Li, D. Zhang, J. Liu, M. Y. Hu, J. Zhao, W. Bi, E. E. Alp, Y. Xiao, and P. Chow
584 (2014), Hidden carbon in Earth's inner core revealed by shear softening in dense Fe7C3,
585 *Proceedings of the National Academy of Sciences*, *111*(50), 17755-17758.

586 Dasgupta, R., and D. Walker (2008), Carbon solubility in core melts in a shallow magma ocean
587 environment and distribution of carbon between the Earth's core and the mantle,
588 *Geochimica et Cosmochimica Acta*, *72*(18), 4627-4641.

589 Dasgupta, R., H. Chi, N. Shimizu, A. S. Buono, and D. Walker (2013), Carbon solution and
590 partitioning between metallic and silicate melts in a shallow magma ocean: Implications
591 for the origin and distribution of terrestrial carbon, *Geochimica et Cosmochimica Acta*,
592 *102*, 191-212.

593 Dubrovinsky, L. S., S. K. Saxena, and P. Lazor (1998), High-pressure and high-temperature in
594 situ X-ray diffraction study of iron and corundum to 68 GPa using an internally heated
595 diamond anvil cell, *Physics and Chemistry of Minerals*, *25*(6), 434-441.

596 Duffy, T.S. and T.J. Ahrens (1993) Thermal expansion of mantle and core materials at very high
597 pressures, *Geophysical Research Letters, 20,* 1103-1106.

598 Dziewonski, A. M., and D. L. Anderson (1981), Preliminary reference Earth model, *Physics of*
599 *the earth and planetary interiors*, *25*(4), 297-356.

600 Fei, Y., and C. Bertka (2005), The interior of Mars, *Science*, *308*(5725), 1120-1121.

Fei, Y., and E. Brosh (2014), Experimental study and thermodynamic calculations of phase relations in the Fe–C system at high pressure, *Earth and Planetary Science Letters*, *408*, 155-162.

Francis, G., and M. Payne (1990), Finite basis set corrections to total energy pseudopotential calculations, *Journal of Physics: Condensed Matter*, *2*(19), 4395.

Garcia, R. F., J. Gagnepain-Beyneix, S. Chevrot, and P. Lognonné (2012), Erratum to "Very Preliminary Reference Moon Model", by RF Garcia, J. Gagnepain-Beyneix, S. Chevrot, P. Lognonné [Phys. Earth Planet. Inter. 188 (2011) 96–113], *Physics of the Earth and Planetary Interiors*, *202*, 89-91.

Hubbell, J., and S. Seltzer (1996), NIST Tables of X-ray Mass Attenuation Coefficients and Mass Energy-Absorption Coefficients from 1 keV to 20MeV for Elements Z= 1 to 92 and 48 Additional Substances of Dosimetric Interest, *National Institute of Standards and Technology, Gaithersburg, MD*.

Jimbo, I., and A. Cramb (1993), The density of liquid iron-carbon alloys, *Metallurgical Transactions B*, *24*(1), 5-10.

Jing, Z., Y. Wang, Y. Kono, T. Yu, T. Sakamaki, C. Park, M. L. Rivers, S. R. Sutton, and G. Shen (2014), Sound velocity of Fe–S liquids at high pressure: Implications for the Moon's molten outer core, *Earth and Planetary Science Letters*, *396*, 78-87.

Kawaguchi, S. I., Y. Nakajima, K. Hirose, T. Komabayashi, H. Ozawa, S. Tateno, Y. Kuwayama, S. Tsutsui, and A. Q. Baron (2017), Sound velocity of liquid Fe-Ni-S at high pressure, *Journal of Geophysical Research: Solid Earth*, *122*(5), 3624-3634.

Kono, Y., C. Park, C. Kenney-Benson, G. Shen, and Y. Wang (2014), Toward comprehensive studies of liquids at high pressures and high temperatures: Combined structure, elastic wave velocity, and viscosity measurements in the Paris–Edinburgh cell, *Physics of the Earth and Planetary Interiors*, *228*, 269-280.

Kresse, G., and J. Furthmüller (1996), Efficiency of ab-initio total energy calculations for metals and semiconductors using a plane-wave basis set, *Computational materials science*, *6*(1), 15-50.

Kuwabara, S., H. Terasaki, K. Nishida, Y. Shimoyama, Y. Takubo, Y. Higo, Y. Shibazaki, S. Urakawa, K. Uesugi, and A. Takeuchi (2016), Sound velocity and elastic properties of Fe–Ni and Fe–Ni–C liquids at high pressure, *Physics and Chemistry of Minerals*, *43*(3), 229-236.

Lai, X., B. Chen, J. Wang, Y. Kono, and F. Zhu (2017), Polyamorphic Transformations in Fe-Ni-C Liquids: Implications for Chemical Evolution of Terrestrial Planets, *Journal of Geophysical Research: Solid Earth*, *122*(12), 9745-9754.

Li, J., and Y. Fei (2014), Experimental constraints on core composition, *Treatise on geochemistry*, *3*, 527-557.

Liu, J.C., J. Li, and D. Ikuta (2016), Elastic softening in Fe7C3 with implications for Earth's deep carbon reservoirs, *Journal of Geophysical Research: Solid Earth*, *121*(3), 1514-1524.

Liu, J., J. F. Lin, V. B. Prakapenka, C. Prescher, and T. Yoshino (2016), Phase relations of Fe3C and Fe7C3 up to 185 GPa and 5200 K: Implication for the stability of iron carbide in the Earth's core, *Geophysical Research Letters*, *43*(24).

Lord, O., M. Walter, R. Dasgupta, D. Walker, and S. Clark (2009), Melting in the Fe–C system to 70 GPa, *Earth and Planetary Science Letters*, *284*(1), 157-167.

Nakajima, Y., E. Takahashi, N. Sata, Y. Nishihara, K. Hirose, K.-i. Funakoshi, and Y. Ohishi (2011), Thermoelastic property and high-pressure stability of Fe7C3: Implication for iron-carbide in the Earth's core, *American Mineralogist*, *96*(7), 1158-1165.

Nakajima, Y., S. Imada, K. Hirose, T. Komabayashi, H. Ozawa, S. Tateno, S. Tsutsui, Y. Kuwayama, and A. Q. Baron (2015), Carbon-depleted outer core revealed by sound velocity measurements of liquid iron–carbon alloy, *Nature communications*, *6*, 8942.

Ogino, K., A. Nishiwaki, and Y. Hosotani (1984), Density of Molten Fe--C Alloys, *J. Jpn. Inst. Met.*, *48*(10), 1004-1010.

Perdew, J. P., J. A. Chevary, S. H. Vosko, K. A. Jackson, M. R. Pederson, D. J. Singh, and C. Fiolhais (1992), Atoms, molecules, solids, and surfaces: Applications of the generalized gradient approximation for exchange and correlation, *Physical review B*, *46*(11), 6671.

Perdew, J. P., A. Ruzsinszky, G. I. Csonka, O. A. Vydrov, G. E. Scuseria, L. A. Constantin, X. Zhou, and K. Burke (2008), Restoring the density-gradient expansion for exchange in solids and surfaces, *Physical review letters*, *100*(13), 136406.

Poirier, J.-P. (1994), Light elements in the Earth's outer core: a critical review, *Physics of the earth and planetary interiors*, *85*(3-4), 319-337.

Prescher, C., L. Dubrovinsky, E. Bykova, I. Kupenko, K. Glazyrin, A. Kantor, C. McCammon, M. Mookherjee, Y. Nakajima, and N. Miyajima (2015), High Poisson's ratio of Earth's inner core explained by carbon alloying, *Nature Geoscience*, *8*(3), 220.

Pronin, L., N. Kazakov, and S. Filippov (1964), Ultrasonic measurements in molten iron, *Izv. Vuzov. Chernaya Metall*, *5*, 12-16.

Sanloup, C., W. Van Westrenen, R. Dasgupta, H. Maynard-Casely, and J.-P. Perrillat (2011), Compressibility change in iron-rich melt and implications for core formation models, *Earth and Planetary Science Letters*, *306*(1-2), 118-122.

Shimoyama, Y., H. Terasaki, E. Ohtani, S. Urakawa, Y. Takubo, K. Nishida, A. Suzuki, and Y. Katayama (2013), Density of Fe-3.5 wt% C liquid at high pressure and temperature and the effect of carbon on the density of the molten iron, *Physics of the Earth and Planetary Interiors*, *224*, 77-82.

Shimoyama, Y., H. Terasaki, S. Urakawa, Y. Takubo, S. Kuwabara, S. Kishimoto, T. Watanuki, A. Machida, Y. Katayama, and T. Kondo (2016), Thermoelastic properties of liquid Fe-C revealed by sound velocity and density measurements at high pressure, *Journal of Geophysical Research: Solid Earth*, *121*(11), 7984-7995.

Steenstra, E. S., Y. Lin, N. Rai, M. Jansen, and W. van Westrenen (2017), Carbon as the dominant light element in the lunar core, *American Mineralogist*, *102*(1), 92-97.

680 Terasaki, H., K. Nishida, Y. Shibazaki, T. Sakamaki, A. Suzuki, E. Ohtani, and T. Kikegawa
681 (2010), Density measurement of Fe3C liquid using X-ray absorption image up to 10 GPa
682 and effect of light elements on compressibility of liquid iron, *Journal of Geophysical*
683 *Research: Solid Earth*, *115*(B6).

684 Terasaki, H., A. Rivoldini, Y. Shimoyama, K. Nishida, S. Urakawa, M. Maki, F. Kurokawa, Y.
685 Takubo, Y. Shibazaki, and T. Sakamaki (2019), Pressure and Composition Effects on
686 Sound Velocity and Density of Core-Forming Liquids: Implication to Core Compositions
687 of Terrestrial Planets, *Journal of Geophysical Research: Planets*, *124*(8), 2272-2293.

688 Wang, J., B. Chen, Q. Williams, and M. Manghnani (2019), Short-and intermediate-range
689 structure and dynamics of Fe-Ni-C liquid under compression, *Frontiers in Earth Science*,
690 *7*, 258.

691 Weber, R. C., P.-Y. Lin, E. J. Garnero, Q. Williams, and P. Lognonne (2011), Seismic detection
692 of the lunar core, *science*, *331*(6015), 309-312.

693 Williams, Q., M. H. Manghnani, R. A. Secco, and S. Fu (2015), Limitations on silicon in the
694 outer core: Ultrasonic measurements at high temperatures and high dK/dP values of Fe-
695 Ni-Si liquids at high pressures, *Journal of Geophysical Research: Solid Earth*, *120*(10),
696 6846-6855.

697 Wood, B. J. (1993), Carbon in the core, *Earth and Planetary Science Letters*, *117*(3-4), 593-607.

698